Editors' Suggestion

Billiards with Spatial Memory

Thijs Albers,* Stijn Delnoij,* Nico Schramma, and Maziyar Jalaal†
Van der Waals–Zeeman Institute, University of Amsterdam, Science Park 904, 1098 XH Amsterdam, The Netherlands

(Received 1 January 2024; accepted 20 March 2024; published 11 April 2024)

Many classes of active matter develop spatial memory by encoding information in space. We present a framework based on mathematical billiards, wherein particles remember their past trajectories. Despite its deterministic rules, such a system is strongly nonergodic and exhibits intermittent statistics and complex pattern formation. We show how these features emerge from the dynamic change of topology. Our work illustrates how the dynamics of a single-body system can dramatically change with spatial memory, laying the groundwork to further explore systems with complex memory kernels.

DOI: 10.1103/PhysRevLett.132.157101

In cognitive psychology, spatial memory refers to the ability to remember and mentally map the physical spaces in the brain [1–6]. It is an essential process in spatial awareness and to reach optimized navigation through complex environments, either for a taxi driver in London to find the fastest route [7,8] or for a mouse to quickly find food in a maze [9]. In fact, a variety of species, from honeybees [10,11] and ants [12] to birds [13], bats [14], and human [1,15], share this cognitive feature. Spatial memory, however, can also be achieved externally: in contrast to a cognitive map (where information is stored internally in the brain), the information is encoded in space itself, and then retrieved when the organism reencounters it. Such memory can potentially enable collective behavior in groups and optimize cost on the organismal level [16,17]. External spatial memory is often mediated by chemical trails and, generally speaking, could be attractive (self-seeking) or repulsive (self-avoiding). Some species of bacteria are attracted to the biochemical trails they leave behind, and by that, they form emergent complex patterns [18–20]. Examples of self-avoiding spatial memory can also be found in the slime mold *Physarum polycephalum*—an eukaryotic multinucleated single cell—which forms spatial memory by leaving extracellular slime at the navigated location while searching for food. The slime then acts as a cue and the cell avoids those regions which have been explored already [21] (see also other memory mechanisms based on vein dilatation and pruning in flow networks [22,23]). Other biological examples can be found in epithelial cell migration when cells modify their external environment by reshaping their extracellular matrix or by secreting biochemical signalling cues [24,25].

The self-avoiding spatial memory is not limited to living systems, but can also be observed in physicochemically self-propelled particles that actively change the energy landscape in which they maneuver. An example is autophoretic active droplets which move due to interfacial stresses caused by surface tension gradients [26–30]. Active droplets leave a chemical trail behind as they move around and avoid these trails due to the local change in concentration gradients. Similar self-avoiding behavior had been observed in other self-propelling active "particles" such as spider molecules [31,32] and even nanoscale surface alloying islands [33].

Understanding and predicting the dynamics of active systems with memories is a difficult task. Most experimental systems are highly nonlinear and include probabilistic features that are often time and material dependent. Additionally, the interaction with the boundaries presents more complexities. Here, we ask the question of how a dynamical system with self-avoiding memory behaves in two dimensions. We present a fully deterministic model with minimal ingredients for motile particles with spatial memory. We report that even such a simple single-body dynamical system exhibits chaos and complex interactions with boundaries, resulting in anomalous dynamics and surprisingly intermittent behavior.

Consider a classical billiard: a massless point particle moves ballistically on a closed two-dimensional domain $\Omega \subset \mathbb{R}^2$. The particle has a constant speed and does not experience any frictional or viscous dissipation. When reaching a boundary $\partial\Omega$, the particle follows an elastic reflection; i.e., the angle of incidence is equal to the angle of reflection.

For over a century, mathematical billiards of various shapes have been studied by physicists and mathematicians to understand dynamical systems and geometries related to various problems, from the theory of heat and light [34,35], and (often Riemannian) surfaces [36–44], to chaos in classical, semiclassical, and quantum systems [45–53].

Here, we present a billiard with memory. In contrast to classical billiards, the particle continuously modifies the topology of the billiard table, creating spatial memory. We consider the simplest type of self-avoiding spatial memory:

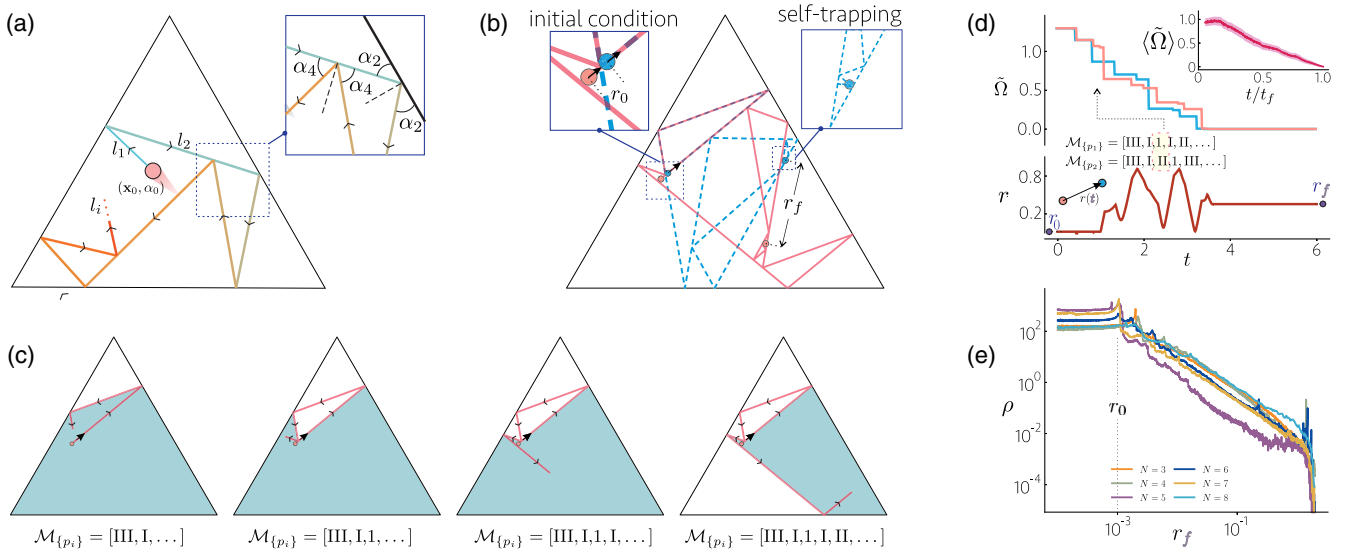

FIG. 1. (a) Underlying principle of self-avoiding billiards. A particle moves ballistically from the initial condition $(\mathbf{x}_0, \alpha_0)$ where $\mathbf{x}_0$ is the initial position vector and α_0 is the initial angle. The particle elastically reflects on the boundaries and its own trajectories, creating a line segment of length l_i, where $i \in [1, \infty)$ is the number of segments. The particle moves until it self-traps in a singular point, where the total length of the trajectory is $\mathcal{L} = \Sigma l_i$ (see Supplemental Material [54], Video 1). (b) Two particles at initially close distance $r_0 = |\mathbf{x}_0^2 - \mathbf{x}_0^1|$ and identical initial angle α_0 diverge significantly from their path and self-trap on distinct locations at a distance r_f (see Supplemental Material, Video 2). (c) A self-avoiding particle changes the effective geometry of the billiard (Ω, highlighted in blue) over time. $\mathcal{M}_{p_i}$ denotes the incident vector of the particle where I, II, and III are the left, bottom, and right edges of the triangle, respectively, and the digits refer to the segment numbers of the trajectory (e.g., 1 for l_1). (d) The dynamics of effective billiard area $\tilde{\Omega}$ and the distance between the two particles r. The inset shows the ensemble average of the effective area versus time normalized by the trapping time t_f. (e) Distribution of r_f for polygons with $\mathcal{N} \in [3, 8]$. In all cases, $r_0 = 10^{-3}$ and the distributions are calculated with 10^5 samples.

the particle reflects on its own trajectories from the past and avoids them in the same way it reflects on the boundaries [see Fig. 1(a) and Supplemental Material [54], Video 1]. This self-avoiding billiard (SAB) features a series of interesting properties. First, it fundamentally lacks periodic orbits (closed geodesics), as the particle cannot follow its past. Second, the particle presents a continuous-time dynamical system with self-induced excluded volume [see Fig. 1(c)]. This means that in the long term the particle reduces the size of its domain $\tilde{\Omega}(t) = \int_\Omega d\mathbf{x}$ by consecutive intersections, i.e., $\tilde{\Omega}(t) \to 0$. Hence, in a SAB, particles have a finite total length $\mathcal{L}$ and eventually trap themselves in singular points in space and time. We refer to this longtime behavior as the *arrested* state. Finally, the topology of a SAB is not fixed as the generated spatial memory dynamically (and dramatically) changes the topology of the surface in a nontrivial manner. Consider a squared table. The topological equivalent surface of a classic square billiard is a torus (easily obtained via the process of *unfolding* [40,62]). A self-avoiding particle generates a singular point at $t = 0$, the moment it is introduced inside the square. As it begins to move ($t > 0$), the singularity (now a line) extends inside the domain, resulting in surfaces with topological genus greater than 1 [42,63]. At some point, the particle forms a new closed domain which is most likely an irrational polygon with an unidentified topological equivalent surface [see Fig. 1(c)].

Importantly, the topological change results in nonergodic characteristics (the particle does not visit everywhere in space, over time) and the anomalous transport of particles and memory-induced chaos: a small change in the initial condition of the particle can drastically change their trajectories as time grows. We demonstrate this in an example shown in Fig. 1(b). The trajectory of the two initially close particles with the same initial angle suddenly separates at the point close to their initial conditions. This bifurcation leads to significantly different trajectories, which eventually self-trap at a distance r_f from each other (see Video 2 in Supplemental Material [54]).

One effective way to categorize the trajectories and demonstrate the chaos in SAB is to record the incidence vector of each particle $\mathcal{M}_{\{p_i\}}$, such that boundaries of the polygons with $\mathcal{N}$ edges are labeled as I, II, III,… and the segments of the trajectories are labeled as $i \in \mathbb{N}$, where $i \geq 1$ [see Fig. 1(c)]. Two initially closed particles have the same incident vector until the bifurcation moment. This is shown in Fig. 1(d) next to the variation of the effective area $\tilde{\Omega}$ around two initially close particles [same as in Fig. 1(b)] and their distance r. The values of $\tilde{\Omega}$ drop every time the particle traps itself in a new polygon, and clearly, $\tilde{\Omega} \to 0$

and $r \to r_f$ as $t \to \infty$ (large number of bounces). Less evident is the probability of r_f for a pair of close particles that are randomly placed in a billiard. Figure 1(e) shows the ensemble-averaged probability density function of r_f for polygons of $N \in [3, 8]$. While the majority of particles stay close to each other, many end up at larger distances, sometimes more than 100 times the initial one. The probability of a larger final distance r_f decays like a power law, approximated as $\rho \sim r_f^{-p}$, where $p \approx 1.4$–1.7 (with a cutoff length set by the maximum length possible in a polygon). The origin of the power-law behavior is yet unclear to us. This class of chaos observed in SAB shares similarities to the concepts of pseudo chaos (also know as weak or slow chaos) [63–66], where singular topological features change the fate of initially close particles, e.g., in Ehrenfest billiard [66] or billiards with barriers [67,68]. A major difference here is that the singular features are induced by the particles themselves and hence depend on the initial particle conditions and the shape of the billiard.

Given the chaotic and self-trapping nature of SAB, a natural question arises: What specific locations in space are particles most likely to become trapped? And how does this likeliness depend on the (initial) geometry of the billiard? To answer these questions, we study self-avoiding rational polygonal billiards with different numbers of edges, $\mathcal{N} \in [3, \infty)$. To this end, we perform computer simulations of 10^8 particles with random initial position vector $(\mathbf{x}_0, \alpha_0)$, where $\mathbf{x}_0$ is the position vector inside Ω and α_0 is the initial angle (see Supplemental Material Sec. A for the details of numerical implementation [54]). Note that the particles do not interact; hence all the present results correspond to a single-body system.

Figure 2(a) shows the probability density function of self-trapped locations $\mathbf{x}_f$ when $t \to \infty$ for the triangular billiard ($\mathcal{N} = 3$). The chaotic properties of SAB result in highly complex and rich patterns. This is associated with sets (modes) of trajectories, some short-lived and some extremely long-lived. This can be seen in the distribution of the total length of the trajectories $\mathcal{L}$, shown in Fig. 2(b) (see Supplemental Material Sec. B for the statistics and calculation of the line segments and incident angles and Supplemental Material Sec. C for illumination and mixing tests [54]).

For simplicity, we analyze this highly intermittent distribution in five different regions (I–V) of total length (an alternative could be to look at sets of particles with similar incident vectors, $\mathcal{M}$; see Supplemental Material Sec. D [54]). Region I belongs to short-lived particles $0 < \mathcal{L} \leq 3$ where the particle self-traps quickly after the movement begins. The majority of these particles trap near the triangular edges. The distribution in region II is different. Particles in this region move for longer distances and form complex structures inside the billiard. These structures suggest the presence of multiple sets of trajectories.

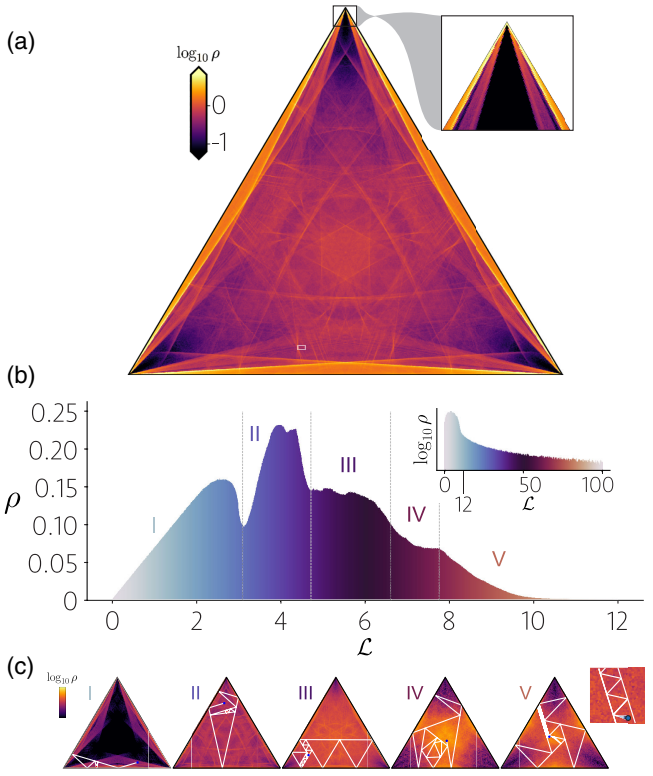

FIG. 2. The arrested state of triangular self-avoiding billiard. (a) Probability density (ρ) of final self-trapping locations. (b) The total length distribution. Inset: semilogarithmic representation to highlight the tail. (c) Distribution of self-trapped positions in regions I–V, shown in (b), and the examples of trajectories of various lengths. The inset on the right shows a magnified view of the zigzag motion in region V. For other polygons, see Supplemental Material Sec. E [54].

Regions I and II include about 60% (29.4% and 29.3%, respectively) of all particles. The rest (regions III–V) are particles with a higher total length, featuring a heavy-tailed distribution [see the inset in Fig. 2(b)]. Particles in these regions generally do not end up near the vertices and *efficiently* use the available space without self-trapping. The rare cases (extreme events) of ultralong trajectories occur in region V. The long lifetime of these particles is a result of a zigzag motion between two almost parallel lines which were previously formed by the particle. Some of these trajectories are 20 times longer than the average trajectory length. However, the probability of their formation is less than 0.03%.

The spatial distribution of the self-trapping positions highly depends on the initial shape of the billiard. Figure 3(a) shows the arrested states for various regular polygons, where the polygons are constructed by choosing $\mathcal{N}$ equidistributed points on a unit circle (see Supplemental Material Sec. E for the counterpart of Fig. 2 for other polygons [54]). The total length distribution of these geometries and also polygons with a higher number of vertices are shown in Fig. 3(b). The dihedral symmetric

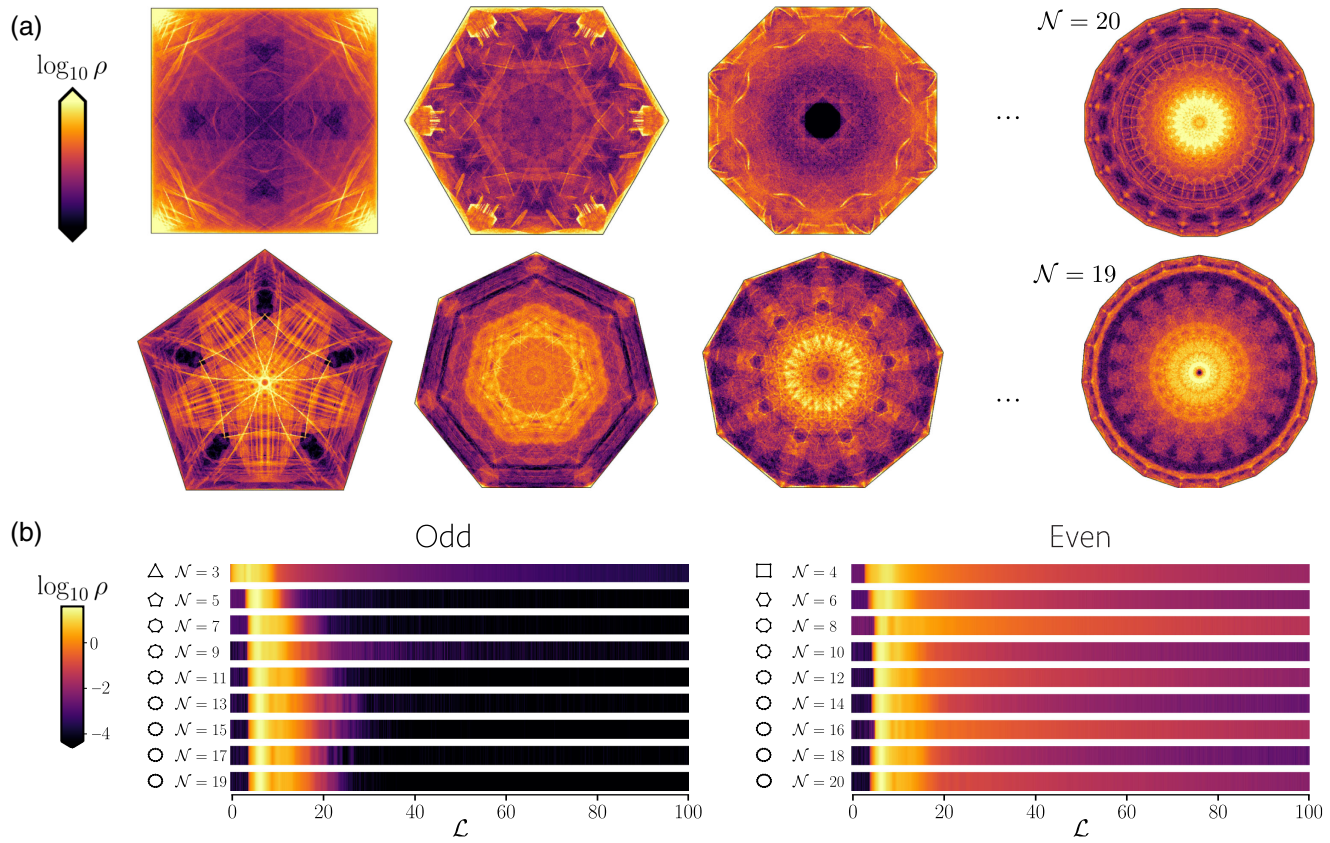

FIG. 3. The arrested state of polygon billiards. (a) Probability density (ρ) of final self-trapping locations in a square, pentagon, hexagon, heptagon, octagon, and nonagon as well as enneadecagon ($\mathcal{N}=19$) and icosagon ($\mathcal{N}=20$). Note that the color bars for each polygon are adjusted to better highlight the distributions. (b) The logarithmic total length distribution for regular polygons of different shapes.

final patterns (with $\mathcal{N}$ rotation and $\mathcal{N}$ reflection symmetries) clearly vary with the geometry of the billiard. But a few features seem to be universal. Particles in even polygons tend to trap more near the vertices and also have a higher chance of a long lifetime ($\mathcal{L}$), since the polygon itself features parallel walls, allowing for zigzag bounces. In contrast, the self-trapping probability in the center is higher for odd polygons, and the probability of a long lifetime is low. Notably, the triangle is the only polygon for which highly likely arbitrarily small orbits are possible since it has interior angles smaller than $\pi/2$. Also remarkably, the odd and even billiards do not converge to a similar distribution even for large values of $\mathcal{N}$, despite that their shapes approach a circle [see Fig. 3 for the comparison of enneadecagon ($\mathcal{N}=19$) and icosagon ($\mathcal{N}=20$)]. This means the effect of parallel walls and the consequent zigzag trajectories remains significant even for large $\mathcal{N}$; hence a long tail persists in the length distribution of even billiards. Note that, the case of a perfect circle features ring patterns in the arrested state, a characteristic expected in a geometry with full continuous symmetry. The details of such rings (location and density), however, remains open to further study (see Supplemental Material Sec. F [54]).

The results presented here illustrate the complex nature of dynamical systems with spatial memory. In contrast to previous studies on active particles with memory (e.g., those used in [69–75]), the current deterministic framework, based on mathematical billiards, employs minimal microscopic rules without noise or particle interaction. Yet, complex patterns and anomalous transport emerge due to memory-induced topological changes.

We found that ballistic particles with spatial memory self-trap and exhibit topology-induced chaos. These dynamical characteristics make it nontrivial to predict the long-time asymptotic behavior of the system. Nonetheless, this limit can be accessed through numerical simulations. As a dynamical system, a SAB fundamentally differs from classic billiards because the surface on which particles flow evolves over time, and the shape of the polygon almost always morphs into an irrational one, which is considerably more challenging to treat mathematically. Nevertheless, the initial shape of the polygon governs the final arrested state, as demonstrated in Fig. 3.

There are several immediate opportunities to extend the findings of this Letter. Classic billiards of different geometries in elliptic or hyperbolic systems (e.g., stadium or

Sinai billiards) may fundamentally exhibit nonergodic and chaotic behavior. Combining spatial memory with such billiards complements the present study. Additionally, in biological or physicochemical systems, spatial memory often dissipates over time as chemical trails diffuse. This introduces another timescale t_m. The ratio of the particle's convective timescale to the fading timescale (known as the Péclet number in hydrodynamics) governs the dynamics of the system. In the current study, $t_m \to \infty$, indicating permanent memory. However, for finite values of t_m, one may observe both self-trapping and untrapping (cage breaking), leading to different long-time behavior and a nonmonotonous trend of the available area $\tilde{\Omega}$. This could also be of particular interest when multiple particles are considered. Moreover, the particle's reaction to its memory and the boundaries represents another control parameter. Here, we consider the simplest form of elastic collision for all interactions. Inelastic collisions [76–79] or probabilistic collisions can significantly alter the system's dynamics. The study of many-body SAB is also of particular interest since particle interactions can take various forms, including reciprocal and nonreciprocal interactions [80–83]. Furthermore, when returning to active biological systems, careful experimentation is needed to study the effects of self-avoiding spatial memory on the motility of these systems. It is important to answer questions such as whether self-trapping occurs in these systems and how biological organisms (e.g., single-celled slime molds, bacteria, or epithelial cells) utilize or avoid self-trapping when changing the landscape around them. Knowledge gained from such experiments can inform additional features of models based on mathematical billiards. Finally, in terms of applications, given the simplicity of the rules employed in this Letter, spatial memory could be utilized to optimize autonomous robotic systems [84,85] and active matter [30,86], especially when combined with learning techniques [87,88].

The authors would like to thank Alvaro Marin and Clélia De Mulatier for insightful discussions.

*These authors contributed equally to this work.
†m.jalaal@uva.nl

[1] E. C. Tolman, Cognitive maps in rats and men, Psychol. Rev. **55**, 189 (1948).
[2] J. O'Keefe and L. Nadel, The Hippocampus as a Cognitive Map (Oxford University Press, 1978).
[3] L. R. Squire, Memory and the hippocampus: A synthesis from findings with rats, monkeys, and humans, Psychol. Rev. **99**, 195 (1992).
[4] H. Eichenbaum, P. Dudchenko, E. Wood, M. Shapiro, and H. Tanila, The hippocampus, memory, and place cells: Is it spatial memory or a memory space?, Neuron **23**, 209 (1999).
[5] B. L. McNaughton, F. P. Battaglia, O. Jensen, E. I. Moser, and M.-B. Moser, Path integration and the neural basis of the 'cognitive map', Nat. Rev. Neurosci. **7**, 663 (2006).
[6] J. O'Keefe, Spatial cells in the hippocampal formation, Nobel Lecture (2014), https://www.nobelprize.org/uploads/2018/06/okeefe-lecture.pdf.
[7] E. A. Maguire, D. G. Gadian, I. S. Johnsrude, C. D. Good, J. Ashburner, R. S. Frackowiak, and C. D. Frith, Navigation-related structural change in the hippocampi of taxi drivers, Proc. Natl. Acad. Sci. U.S.A. **97**, 4398 (2000).
[8] K. Woollett, H. J. Spiers, and E. A. Maguire, Talent in the taxi: A model system for exploring expertise, Phil. Trans. R. Soc. B **364**, 1407 (2009).
[9] S. Sharma, S. Rakoczy, and H. Brown-Borg, Assessment of spatial memory in mice, Life Sci. **87**, 521 (2010).
[10] R. Menzel, U. Greggers, A. Smith, S. Berger, R. Brandt, S. Brunke, G. Bundrock, S. Hülse, T. Plümpe, F. Schaupp *et al.*, Honey bees navigate according to a map-like spatial memory, Proc. Natl. Acad. Sci. U.S.A. **102**, 3040 (2005).
[11] M. Collett, L. Chittka, and T. S. Collett, Spatial memory in insect navigation, Curr. Biol. **23**, R789 (2013).
[12] Y. Heyman, Y. Vilk, and O. Feinerman, Ants use multiple spatial memories and chemical pointers to navigate their nest, Iscience **14**, 264 (2019).
[13] S. D. Healy and T. A. Hurly, Spatial learning and memory in birds, Brain Behav. Evol. **63**, 211 (2004).
[14] M. M. Yartsev and N. Ulanovsky, Representation of three-dimensional space in the hippocampus of flying bats, Science **340**, 367 (2013).
[15] N. Burgess, Spatial memory: How egocentric and allocentric combine, Trends Cognit. Sci. **10**, 551 (2006).
[16] G. Cabanes, E. van Wilgenburg, M. Beekman, and T. Latty, Ants build transportation networks that optimize cost and efficiency at the expense of robustness, Behav. Ecol. **26**, 223 (2015).
[17] J. Smith-Ferguson, C. R. Reid, T. Latty, and M. Beekman, Hänsel, Gretel and the slime mould—How an external spatial memory aids navigation in complex environments, J. Phys. D **50**, 414003 (2017).
[18] E. O. Budrene and H. C. Berg, Complex patterns formed by motile cells of escherichia coli, Nature (London) **349**, 630 (1991).
[19] E. O. Budrene and H. C. Berg, Dynamics of formation of symmetrical patterns by chemotactic bacteria, Nature (London) **376**, 49 (1995).
[20] N. Mittal, E. O. Budrene, M. P. Brenner, and A. Van Oudenaarden, Motility of *Escherichia coli* cells in clusters formed by chemotactic aggregation, Proc. Natl. Acad. Sci. U.S.A. **100**, 13259 (2003).
[21] C. R. Reid, T. Latty, A. Dussutour, and M. Beekman, Slime mold uses an externalized spatial "memory" to navigate in complex environments, Proc. Natl. Acad. Sci. U.S.A. **109**, 17490 (2012).
[22] M. Kramar and K. Alim, Encoding memory in tube diameter hierarchy of living flow network, Proc. Natl. Acad. Sci. U.S.A. **118**, e2007815118 (2021).
[23] K. Bhattacharyya, D. Zwicker, and K. Alim, Memory formation in adaptive networks, Phys. Rev. Lett. **129**, 028101 (2022).

[24] J. D'alessandro, A. Barbier-Chebbah, V. Cellerin, O. Benichou, R. M. Mège, R. Voituriez, and B. Ladoux, Cell migration guided by long-lived spatial memory, Nat. Commun. **12**, 4118 (2021).

[25] A. G. Clark, A. Maitra, C. Jacques, M. Bergert, C. Pérez-González, A. Simon, L. Lederer, A. Diz-Muñoz, X. Trepat, R. Voituriez *et al.*, Self-generated gradients steer collective migration on viscoelastic collagen networks, Nat. Mater. **21**, 1200 (2022).

[26] S. Thutupalli, R. Seemann, and S. Herminghaus, Swarming behavior of simple model squirmers, New J. Phys. **13**, 073021 (2011).

[27] P. G. Moerman, H. W. Moyses, E. B. van der Wee, D. G. Grier, A. van Blaaderen, W. K. Kegel, J. Groenewold, and J. Brujic, Solute-mediated interactions between active droplets, Phys. Rev. E **96**, 032607 (2017).

[28] C. Jin, C. Krüger, and C. C. Maass, Chemotaxis and autochemotaxis of self-propelling droplet swimmers, Proc. Natl. Acad. Sci. U.S.A. **114**, 5089 (2017).

[29] B. V. Hokmabad, R. Dey, M. Jalaal, D. Mohanty, M. Almukambetova, K. A. Baldwin, D. Lohse, and C. C. Maass, Emergence of bimodal motility in active droplets, Phys. Rev. X **11**, 011043 (2021).

[30] B. V. Hokmabad, J. Agudo-Canalejo, S. Saha, R. Golestanian, and C. C. Maass, Chemotactic self-caging in active emulsions, Proc. Natl. Acad. Sci. U.S.A. **119**, e2122269119 (2022).

[31] R. Pei, S. K. Taylor, D. Stefanovic, S. Rudchenko, T. E. Mitchell, and M. N. Stojanovic, Behavior of polycatalytic assemblies in a substrate-displaying matrix, J. Am. Chem. Soc. **128**, 12693 (2006).

[32] P. E. Hamming, N. J. Overeem, and J. Huskens, Influenza as a molecular walker, Chem. Sci. **11**, 27 (2020).

[33] A. Schmid, N. Bartelt, and R. Hwang, Alloying at surfaces by the migration of reactive two-dimensional islands, Science **290**, 1561 (2000).

[34] L. Kelvin, I. Nineteenth century clouds over the dynamical theory of heat and light, London, Edinburgh, Dublin Philos. Mag. J. Sci. **2**, 1 (1901).

[35] Y. G. Sinai, *Ergodic Theory* (Springer, New York, 1973).

[36] W. A. Veech, Teichmüller curves in moduli space, Eisenstein series and an application to triangular billiards, Inventiones Mathematicae **97**, 553 (1989).

[37] S. Kerckhoff, H. Masur, and J. Smillie, Ergodicity of billiard flows and quadratic differentials, Ann. Math. **124**, 293 (1986).

[38] E. Gutkin, Billiard dynamics: An updated survey with the emphasis on open problems, Chaos **22**, 026116 (2012).

[39] A. Eskin and M. Mirzakhani, Invariant and stationary measures for the action on moduli space, Publ. Math. l'IHÉS **127**, 95 (2018).

[40] A. Wright, From rational billiards to dynamics on moduli spaces, Bull. Am. Math. Soc. **53**, 41 (2016).

[41] A. Eskin, C. McMullen, R. Mukamel, and A. Wright, Billiards quadrilaterals and moduli spaces, J. Am. Math. Soc. **33**, 1039 (2020).

[42] E. Gutkin, Billiards on almost integrable polyhedral surfaces, Ergod. Theory Dyn. Syst. **4**, 569 (1984).

[43] C. McMullen, Billiards and Teichmüller curves on Hilbert modular surfaces, J. Am. Math. Soc. **16**, 857 (2003).

[44] K. Fraczek and C. Ulcigrai, Non-ergodic-periodic billiards and infinite translation surfaces, Inventiones Mathematicae **197**, 241 (2014).

[45] M. V. Berry, Quantizing a classically ergodic system: Sinai's billiard and the KKR method, Ann. Phys. (N.Y.) **131**, 163 (1981).

[46] E. J. Heller, Bound-state eigenfunctions of classically chaotic Hamiltonian systems: Scars of periodic orbits, Phys. Rev. Lett. **53**, 1515 (1984).

[47] S. Tomsovic and E. J. Heller, Long-time semiclassical dynamics of chaos: The stadium billiard, Phys. Rev. E **47**, 282 (1993).

[48] J. U. Nöckel and A. D. Stone, Ray and wave chaos in asymmetric resonant optical cavities, Nature (London) **385**, 45 (1997).

[49] C. Dembowski, H.-D. Gräf, A. Heine, R. Hofferbert, H. Rehfeld, and A. Richter, First experimental evidence for chaos-assisted tunneling in a microwave annular billiard, Phys. Rev. Lett. **84**, 867 (2000).

[50] A. D. Stone, Chaotic billiard lasers, Nature (London) **465**, 696 (2010).

[51] M. Serbyn, D. A. Abanin, and Z. Papić, Quantum many-body scars and weak breaking of ergodicity, Nat. Phys. **17**, 675 (2021).

[52] J. Ravnik, Y. Vaskivskyi, J. Vodeb, P. Aupič, I. Vaskivskyi, D. Golež, Y. Gerasimenko, V. Kabanov, and D. Mihailovic, Quantum billiards with correlated electrons confined in triangular transition metal dichalcogenide monolayer nanostructures, Nat. Commun. **12**, 3793 (2021).

[53] Č. Lozej, G. Casati, and T. Prosen, Quantum chaos in triangular billiards, Phys. Rev. Res. **4**, 013138 (2022).

[54] See Supplemental Material at http://link.aps.org/supplemental/10.1103/PhysRevLett.132.157101, which includes Refs. [55–61], for additional information about the method and a detailed discussion of the computational results.

[55] J. Bezanson, A. Edelman, S. Karpinski, and V. B. Shah, Julia: A fresh approach to numerical computing, SIAM Rev. **59**, 65 (2017).

[56] G. Datseris, DynamicalBilliards.jl: An easy-to-use, modular and extendable Julia package for dynamical billiard systems in two dimensions, J. Open Source Software **2**, 458 (2017).

[57] V. Klee, Is every polygonal region illuminable from some point?, Am. Math. Mon. **76**, 180 (1969).

[58] G. W. Tokarsky, Polygonal rooms not illuminable from every point, Am. Math. Mon. **102**, 867 (1995).

[59] S. Lelievre, T. Monteil, and B. Weiss, Everything is illuminated, Geom. Topol. **20**, 1737 (2016).

[60] A. Wolecki, Illumination in rational billiards, arXiv:1905.09358.

[61] Numberphile, The illumination problem, Youtube Channel (2017), https://www.youtube.com/@numberphile.

[62] H. Masur and S. Tabachnikov, Rational billiards and flat structures, in *Handbook of Dynamical Systems* (Elsevier, New York, 2002), Vol. 1, pp. 1015–1089.

[63] P. Richens and M. Berry, Pseudointegrable systems in classical and quantum mechanics, Physica (Amsterdam) **2D**, 495 (1981).

[64] G. Zaslavsky and M. Edelman, Pseudochaos, *Perspectives and Problems in Nolinear Science: A Celebratory Volume in Honor of Lawrence Sirovich* (Springer, 2003) p. 421.

[65] R. Klages, Weak chaos, infinite ergodic theory, and anomalous dynamics, *From Hamiltonian Chaos to Complex Systems: A Nonlinear Physics Approach*, (Springer, 2013) p. 3.
[66] C. Ulcigrai, Slow chaos in surface flows, Boll. Unione Mat. Ital. **14**, 231 (2021).
[67] A. Eskin, H. Masur, and M. Schmoll, Billiards in rectangles with barriers, Duke Math. J. **120**, 427 (2003).
[68] B. Carreras, V. Lynch, L. Garcia, M. Edelman, and G. Zaslavsky, Topological instability along filamented invariant surfaces, Chaos **13**, 1175 (2003).
[69] B. Schulz, S. Trimper, and M. Schulz, Feedback-controlled diffusion: From self-trapping to true self-avoiding walks, Phys. Lett. A **339**, 224 (2005).
[70] W. T. Kranz and R. Golestanian, Trail-mediated self-interaction, J. Chem. Phys. **150**, 214111 (2019).
[71] A. Gelimson, K. Zhao, C. K. Lee, W. T. Kranz, G. C. L. Wong, and R. Golestanian, Multicellular self-organization of *P. aeruginosa* due to interactions with secreted trails, Phys. Rev. Lett. **117**, 178102 (2016).
[72] W. T. Kranz, A. Gelimson, K. Zhao, G. C. L. Wong, and R. Golestanian, Effective dynamics of microorganisms that interact with their own trail, Phys. Rev. Lett. **117**, 038101 (2016).
[73] A. Sengupta, S. van Teeffelen, and H. Löwen, Dynamics of a microorganism moving by chemotaxis in its own secretion, Phys. Rev. E **80**, 031122 (2009).
[74] K. Daftari and K. A. Newhall, Self-avoidant memory effects on enhanced diffusion in a stochastic model of environmentally responsive swimming droplets, Phys. Rev. E **105**, 024609 (2022).
[75] A. Barbier-Chebbah, O. Bénichou, and R. Voituriez, Self-interacting random walks: Aging, exploration, and first-passage times, Phys. Rev. X **12**, 011052 (2022).
[76] S. E. Spagnolie, C. Wahl, J. Lukasik, and J.-L. Thiffeault, Microorganism billiards, Physica (Amsterdam) **341D**, 33 (2017).
[77] C. Eyles, M. Brouard, C.-H. Yang, J. Kłos, F. Aoiz, A. Gijsbertsen, A. Wiskerke, and S. Stolte, Interference structures in the differential cross-sections for inelastic scattering of NO by Ar, Nat. Chem. **3**, 597 (2011).
[78] A. Théry, Y. Wang, M. Dvoriashyna, C. Eloy, F. Elias, and E. Lauga, Rebound and scattering of motile chlamydomonas algae in confined chambers, Soft Matter **17**, 4857 (2021).
[79] M. Besemer, G. Tang, Z. Gao, A. van der Avoird, G. C. Groenenboom, S. Y. van de Meerakker, and T. Karman, Glory scattering in deeply inelastic molecular collisions, Nat. Chem. **14**, 664 (2022).
[80] M. Durve, A. Saha, and A. Sayeed, Active particle condensation by non-reciprocal and time-delayed interactions, Eur. Phys. J. E **41**, 1 (2018).
[81] C. H. Meredith, P. G. Moerman, J. Groenewold, Y.-J. Chiu, W. K. Kegel, A. van Blaaderen, and L. D. Zarzar, Predator–prey interactions between droplets driven by non-reciprocal oil exchange, Nat. Chem. **12**, 1136 (2020).
[82] K. L. Kreienkamp and S. H. Klapp, Clustering and flocking of repulsive chiral active particles with non-reciprocal couplings, New J. Phys. **24**, 123009 (2022).
[83] S. Osat and R. Golestanian, Non-reciprocal multifarious self-organization, Nat. Nanotechnol. **18**, 79 (2023).
[84] W. Burgard, M. Moors, D. Fox, R. Simmons, and S. Thrun, Collaborative multi-robot exploration, in *Proceedings of the 2000 IEEE International Conference on Robotics and Automation, Millenium Conference* (IEEE, New York, 2000), Cat. No. 00CH37065, Vol. 1, pp. 476–481.
[85] C. Garcia-Saura, E. Serrano, F. B. Rodriguez, and P. Varona, Intrinsic and environmental factors modulating autonomous robotic search under high uncertainty, Sci. Rep. **11**, 24509 (2021).
[86] B. Nakayama, H. Nagase, H. Takahashi, Y. Saito, S. Hatayama, K. Makino, E. Yamamoto, and T. Saiki, Tunable pheromone interactions among microswimmers, Proc. Natl. Acad. Sci. U.S.A. **120**, e2213713120 (2023).
[87] L. P. Kaelbling, The foundation of efficient robot learning, Science **369**, 915 (2020).
[88] A. Ecoffet, J. Huizinga, J. Lehman, K. O. Stanley, and J. Clune, First return, then explore, Nature (London) **590**, 580 (2021).